Biomimetic strategy to reversibly trigger functionality of catalytic nano-compartments by insertion of pH-responsive bio-valves

Journal:	*Nano Letters*
Manuscript ID	nl-2017-02886m.R4
Manuscript Type:	Communication
Date Submitted by the Author:	29-Aug-2017
Complete List of Authors:	Edlinger, Christoph; University of Basel Einfalt, Tomaz; University Basel, Chemistry Department Spulber, Mariana; University of Basel, Chemistry Department Car, Anja; University of Basel, Meier, Wolfgang; University of Basel, Department of Chemistry Palivan, Cornelia; University of Basel, Chemistry Department

Biomimetic strategy to reversibly trigger functionality of catalytic nano-compartments by insertion of pH-responsive bio-valves

Christoph Edlinger[1], Tomaz Einfalt[1], Mariana Spulber[1], Anja Car[1], Wolfgang Meier[1*], Cornelia G. Palivan[1*]

[1]Department of Chemistry, University of Basel, Klingelbergstrasse 80 CH-4056 Basel, Switzerland

Corresponding Author

*E-mail: cornelia.palivan@unibas.ch; wolfgang.meier@unibas.ch

Fax: +41 (0)61 2073855; Phone: +41 (0) 61 2073839 and +41 (0) 61 2073802.

Abstract: We describe an innovative strategy to generate catalytic compartments with triggered functionality at the nanoscale level by combining pH-reversible bio-valves and enzyme-loaded synthetic compartments. The bio-valve has been engineered by attachment of stimuli-responsive peptides to a genetically modified channel porin, enabling a reversible change of the molecular flow through the pores of the porin in response to a pH change in the local environment. The bio-valve functionality triggers the reaction inside the cavity of the enzyme-loaded compartments by switching the *in situ* activity of the enzymes on/off based on a reversible change of the permeability of the membrane, which blocks or allows the passage of substrates and products. The complex functionality of our catalytic compartments is based on preservation of the integrity of the compartments to protect encapsulated enzymes. An increase of the *in situ* activity compared to that of the free enzyme, and a reversible on/off switch of the activity upon the presence of a specific stimulus is achieved. This strategy provides straightforward solutions for development of catalytic nanocompartments efficiently producing desired molecules in a controlled, stimuli-responsive manner with high potential in areas, such as medicine, analytical chemistry, and catalysis.

Keywords: stimuli-responsiveness; catalytic nanocompartment; membrane-protein; triggered bio-activity; reversible permeability

In nature, controlled transport of molecules between cellular and subcellular compartments is vital for functional cellular metabolism and is achieved via delicate molecular mechanisms involving membrane proteins (MPs). A plethora of MPs located in cellular phospholipid bilayers allow active or passive transport of molecules through the compartment membrane. Such molecular transport is frequently triggered by stimuli such as pH or temperature change, transmembrane potential, light, or the presence of specific molecules.[1-3] A bioinspired strategy on focus today for development of new materials is based on interfacing biomolecules such as MPs, enzymes, and proteins with synthetic membranes (planar membranes and compartments).[4, 5] Such bio-nanoassemblies combine the activity of biomolecules with the architecture of a synthetic assembly, generating new materials with emergent properties and functionality that have high potential in various domains of technology, medicine and environmental sciences.[5-7] Bio-nanoassemblies have been designed as models in order to understand the activity of biomolecules in synthetic matrixes proposed as artificial organelles,[8, 9] molecular motors,[10] and simple models of artificial cells.[11] In addition, bio-nanoassemblies have been developed for applications, such as local synthesis of polymers,[12] active surfaces serving for production of antibiotics[13] or sensitive biosensing,[14] and membranes for water purification.[15]

Particularly interesting are catalytic compartments named nanoreactors which are based on encapsulation of active compounds (proteins, enzymes, mimics) in the cavity of compartments where they are able to fulfil their function of protected reactions at the nanoscale.[5, 16] These catalytic compartments can be used to study enzymatic reactions in confined spaces, or for specific applications such as detoxification of reactive oxygen species and storage of oxygen,[17] enzyme-mediated biotransformation,[18] synthesis of polymers,[12] or even as simple mimics of cell organelles.[19-21] Polymer vesicles are particularly appealing compartments, with sizes ranging from nanometers (polymersomes) up to micrometers (synthetic giant unilamellar vesicles, synthetic GUVs). In comparison to liposomes (lipid

based compartments closely related to cell membranes), polymer compartments have specific advantages arising from the intrinsic chemical nature of the polymers: i) greater mechanical stability, ii) tunable membrane properties (thickness, flexibility, composition), and iii) ability to be functionalized with different molecular groups.[22-24] Appropriately selected amphiphilic copolymers that self-assemble into polymersomes or GUVs can be both nontoxic and responsive, changing their architecture in the presence of a specific stimulus, properties largely exploited for development of drug delivery systems.[25] However in the case of the catalytic compartments, it is not possible to use stimuli-responsive polymers that change their architecture, because their irreversible disassembly would lead to the release of the active compounds.[26, 27]

Membrane permeability is an essential property for *in situ* reactions inside catalytic compartments, to allow the reaction substrates to pass inside and products to be released. Polymer membranes have been rendered permeable by various approaches: i) using copolymers which generate porous membranes,[28-30] ii) inducing pores by chemical treatment,[12, 18, 31] or iii) mimicking cell membranes by insertion of biopores and MPs.[6] Once reconstituted in polymersome membranes, MPs such as AqpZ, LamB, OmpF, Tsx and FhuA[6, 32, 33] and membrane penetrating peptides such as gramicidin[34, 35] allow diffusion of ions and small molecular weight molecules with a selectivity based on their intrinsic properties. In order to develop stimuli-responsive compartments that preserve their architecture as well as support *in situ* reactions, a biomimetic approach is to use appropriate MPs to induce responsiveness. To date only a few liposome and polymersome membranes have been permeabilized by insertion of modified channel proteins that possess stimuli-responsiveness.[36, 37] The membrane proteins have been modified to equip them with a cleavable responsive molecular cap, which is cleaved in the presence of a specific stimulus, and the molecular flow through the pore is restored. Stimuli responsive protein pores were

designed to react to external changes in pH (OmpF,[36, 38] MS-CL[39]) or reduction potential (FhuA[40, 41]). Another approach to obtain stimuli responsive MPs is based on using amino acid mutations, to create charge repulsion in the channel interior (OmpF),[38] or introduce an elastin-like polypeptide loop with temperature triggered solubility.[42] A more appealing approach for practical applications, which involves a permanent attachment of a stimuli responsive molecular group, has been applied only to ion channels.[43, 44] Unfortunately, such engineered ion channels cannot be used as "gates" for catalytic compartments, because they do not allow the diffusion of small molecular weight enzymatic substrates.

We introduce here a biomimetic strategy to develop catalytic compartments with controlled functionality triggered in a stimuli-responsive manner by changes in the compartments environment. The catalytic compartments with reversibly triggered activity are obtained by introducing into the synthetic membrane of enzyme-loaded polymersomes bio-valves based on modified membrane proteins. Bio-valves were engineered by attaching molecules able to change the conformation and properties of channel porins in specific conditions. These attached molecules enable reversible opening and closing of the porin pores, depending on environmental conditions. Such bio-valves can efficiently switch on/off *in situ* activity when inserted in the membrane of the compartments (Figure 1). We selected OmpF as a model channel porin, because of its well characterised crystal structure, remarkable stability (temperature, solvents, detergents and pH),[38, 45, 46] and moderate pore size, allowing molecules of up to 600 Da to pass through.[38, 46] In order to favour the attachment of a molecular cap, we genetically engineered OmpF through point mutation to feature two cysteine residues in specific positions on the channel interior (OmpF-M), and then attached a peptide to those cysteines. Changes in pH induce this peptide to make reversible conformational changes and thus block (closed state) or unblock (open state) the pore of the peptide-OmpF-M conjugate (OmpF-C). OmpF-C was inserted into the membrane of polymersomes based on poly(2-

methyl-2-oxazoline)-block- poly(dimethylsiloxane)-block poly(2-methyl-2-oxazoline) (PMOXA-*b*-PDMS-*b*-PMOXA) loaded with Horseradish Peroxidase (HRP). We selected PMOXA- *b*-PDMS- *b*-PMOXA amphiphilic triblock copolymers for self-assembly into polymersomes because of their flexible membranes and previously reported ability to successfully incorporate MPs.[47] *In situ* activity of HRP was followed during reversible changes in pH to evaluate the open/close functionality of OmpF-C.

Our approach is a resourceful strategy to design a reversible gating system that it is not restricted to a single "activation" of the catalytic compartment by opening the pores but can be switched on and off over several cycles, potentially maintaining stimuli-responsiveness for long-term utilization. Both, a reversible and precise response in time and space upon an external stimulus and the large variety of possible applications by encapsulation of appropriate active compounds (enzyme, proteins, mimics) highlight the potential of our system in areas such as medicine, catalysis, and technology, where such materials will provide desired processes/compounds "on demand".

To induce stimuli responsiveness of the OmpF porin, we attached a pH-responsive peptide capable of significant changes in charge and conformation upon changes of pH from 7.4 to 6.0. Each of the pH-responsive amino acid groups must be accompanied by hydrophobic amino acids, in order to create a more pronounced change in solubility between different protonation states, and to be obtained by a straightforward synthesis and purification procedure. An example of a peptide sequence that meets these requirements is GALA (WEAALAEALAEALAEHLAEALAEALEALAA), previously reported to change its polarity and conformation producing two distinct states pH 5.5 and 7.5.[48] In addition, the peptide sequence has to be adapted to the geometric constrains of the elliptical OmpF pore with an inner diameter of 7-11 Å.[46]

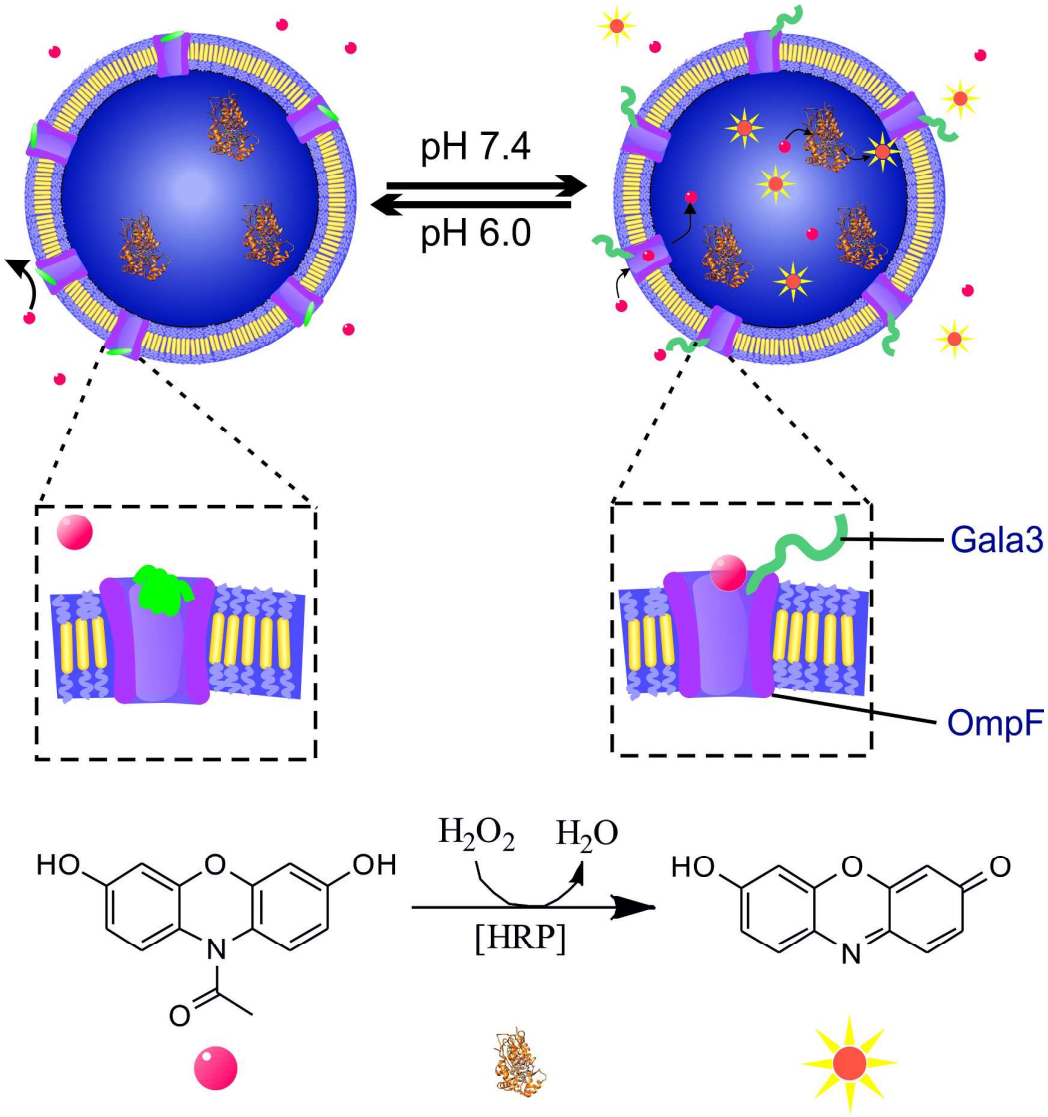

Figure 1. Schematic representation of a bio-valve functioning by reversible pore opening and closing inside the membrane of nanocompartments to trigger an *in situ* reaction (left: closed state; right open state). Modified OmpF pore (purple; stimuli responsive group green) is inserted in the polymersome membrane that separates the encapsulated enzyme (HRP) from the environment. The *in situ* reaction is triggered by the bio-valve functionality, which allows the diffusion through the OmpF pores of the substrate Amplex UltraRed® (magenta spheres) and the subsequent release of the fluorescent products (yellow stars).

Only peptides with a total length of 20-50 Å are suitable to block the pore, considering that both random coil and α-helix structures are significantly shorter than the corresponding stretched peptide (Figure 2). In this respect, a GALA sequence shortened to LAEALAEALAEA (Gala3) is an optimum peptide sequence matching the requirement of closing the OmpF pore, and thus we selected it for this purpose. In order to allow a significant change in protonation, at least three carboxylic acids were incorporated in the peptide structure. Considering the neighbouring hydrophobic amino acids, the minimal length requirement for the peptide sequence is indeed obtained with Gala3.

In order to attach the responsive peptide to the channel protein, first OmpF was genetically modified to introducing cysteine residues at key locations in the OmpF amino acid sequence. The mutation sites K89C (lysine) and R270C (arginine) located inside the pore in the eyelet-region were replaced by cysteines (Figure 2) as anchoring points for the attachment of molecular groups that can block the molecular flow at the beginning of the pore or point outwards without obstructing the pore, in different conditions. (Figure 2B) 3D representations of OmpF-C (Figure 2C) were obtained using Pymol and the crystal structure of OmpF wild type from the RSCB Protein database with the cysteines residues attached. We used two mutations in order to increase the labelling efficiency of the porin, and to offer better conditions to block the OmpF pore because two peptides will occupy more space inside the pore.

The mutation was performed via polymerase chain reaction (PCR) of the entire plasmid. The K89C-mutation was introduced first, and then the R270C-mutation was introduced by the same procedure. The plasmid was shifted to higher masses than the template (unmodified plasmid), which remained supercoiled (Figure S1). After purification via gel-electrophoresis, the PCR product was isolated and sequenced, confirming the mutation (Table S2, Supporting Information). The double mutant of the porin, K89C-R270C-OmpF (OmpF-M) was then overexpressed in Omp8 E.coli. Its excess over naturally occurring OmpF-WT made further

separation unnecessary. OmpF-M could not be distinguished on gel from OmpF-WT or single mutants K89C-OmpF and R270C-OmpF, indicating a successful expression and good purity, because of the lack of additional bands in the Coomassie stained gel (Figure S2, S3, Supporting Information). The occasionally observed splitting of the OmpF band (Figure S2) is attributed to the presence of residual signalling peptide (2000 Da).[49] An OmpF-M concentration of 0.75±0.25mg/mL (extract without further concentration steps) was determined by BCA total protein assay®. The presence of thiol groups and their accessibility was evaluated by binding them with the thiol-reactive fluorophore acrylodane. As expected, OmpF-WT did not reveal any fluorescence intensity upon addition of acrylodane, indicating the lack of nonspecific binding of the fluorophore to the porin. On the contrary, the fluorescence intensity of acrylodane when added to the thiol-bearing mutants (K89C-OmpF, R270C-OmpF and OmpF-M), clearly indicates successful thio-functionalization of the porin. Moreover, the fluorescence intensity of acrylodane when bound to the double mutant OmpF-M was similar to that resulting from a double concentration of R270C-OmpF bound to acrylodane (Figure S5, Supporting Information), indicating that both thiol groups are accessible, and can bind to small molecular weight molecules. To attach Gala3 to the thiols of the cysteine residues in the OmpF-M, Michael addition was chosen due to its straightforward approach, fewer side-reactions compared to disulphide bonds formation with the cysteine residues, or to direct alkylation of the cysteine residues with halogenoalkanes.[50, 51] In addition, the chosen glycine maleic imide linker between OmpF-M and Gala3 is a small molecule (97 Da) and expected to have no impact on substrate translocation through the pore due to its small size.

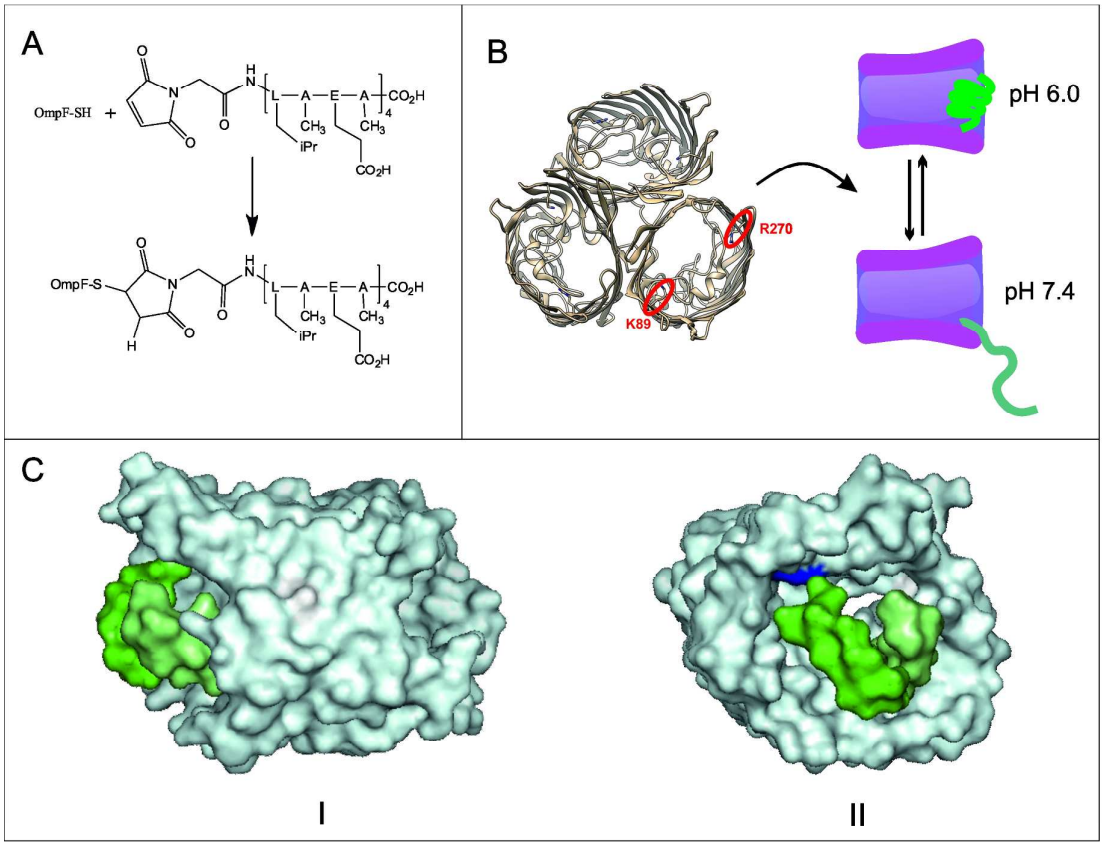

Figure 2. A. Michael addition of the Gala3 peptide to the cysteine side chains of the OmpF-M; B. Location of the mutation sites K89 and R270 (highlighted only in one of the three channels of the OmpF trimer) and a schematic representation of the cross-section of the pore in "closed state", with Gala3 blocking the entrance of the pore (above) and in "open state", with the attached Gala3 freely moving in its random-coil state (below). C. Three-dimensional representation of OmpF-C after binding of the pH responsive peptide Gala3 (green) attached in helical structure (compact state) to cysteine residues (blue) of OmpF-M showing closing of the pore: view from the side (I), and from the top (II).

The degree of labelling (DOL) of the double mutant OmpF-M with Gala3 (OmpF-C) was determined using a combination of mass spectrometry (MS), and the acrylodane assay. For

the prior, OmpF-C and OmpF-M were purified via SDS-gel electrophoresis and digested within the gel, resulting in various peptides. Mass spectroscopy is a direct and absolute method for quantification, however, long hydrophobic peptides are particularly difficult to ionize and transfer into the gas phase. Such peptide sequences are typical for membrane proteins such as OmpF.[52] Thus it was necessary to perform an indirect measurement by comparing the ratio between the intensities of the mass peaks of the cysteine-bearing OmpF fragment without Gala3 with another peptide without cysteine, and calibrating it with OmpF-M. (Equation 2; Supporting Information) This eliminated the dependency on the protein concentration, as the other peptide served as an internal standard. The measurements indicate that 94% ± 5% of the thiol groups within the double mutant OmpF-M bound Gala 3 (92% ± 5% of K89C- and 96% ± 5% of R270C anchor points had the Gala3 peptide attached) (Table S3). We used as a complementary qualitative assay, the acrylodane assay, which is based on binding of acrylodane to the accessible thiol groups that remain unbound after the attachment of Gala3. A DOL value of 68% ± 9% was obtained, indicating a successful binding of Gala3 to the modified OmpF (Figure S4, Supporting Information, Table S4**)**. DOL value determined with the acrylodane assay was lower than determined by mass spectroscopy due to fluorophore interactions with aromatic amino acid residues.[53, 54] However, both MS and the acrylodane assay indicate successful thio-functionalization of the OmpF-M, as an essential step for the attachment of Gala3.

A second step in obtaining reversible pH-responsive catalytic compartments was to insert OmpF-C into polymersome membranes together with simultaneous encapsulation of an enzyme inside the cavity, and then to test the overall functionality. We used the rehydration method to generate catalytic compartments,[55] NR, by self-assembly of $PMOXA_6$-*b*-$PDMS_{44}$-*b*-$PMOXA_6$ amphiphilic block copolymers in the presence of: HRP (NR-), HRP and OmpF-C (NRC), and HRP OmpF-M (NR+). OmpF-C/-M were directly added to an ethanolic copolymer solution before drying until a thin polymer film was formed. Slow hydration with

biomolecule solutions in PBS induced the self-assembly process and formation of polymersomes containing the biomolecules in specific locations depending of their intrinsic character: OmpF-C/-M in the membrane, with HRP inside the cavity. In general, the efficiency and homogeneity of polymersome formation, and OmpF insertion depend on numerous factors, as for example the presence of surfactants, such as octylglucopyranoside (OG), used in the membrane protein extraction and stabilisation.[56] (Figure S9, Supporting Information). Since OG was only required for the initial steps of OmpF extraction and the stabilisation in solution, its concentration was reduced to the minimal possible concentration for storage (0.5 w/w %), and was further removed prior to mixing it with the copolymer solution. Before dialysis, polymersome size was controlled by extrusion through 0.2 μm polycarbonate filters. Polymersome solutions were diluted to the same concentration (determined by their respective ability to scatter light). The final polymersome concentration was considered as the lowest concentration determined for NR-, NRC and NR+. The homogeneity of the polymersomes size was confirmed by dynamic light scattering as with a PDI < 0.2.

The size and the architecture of the polymer assemblies resulting from the self-assembly of the copolymers without and with the biomolecules were determined by static and dynamic light scattering, SLS and DLS (Table 1; Figure S6-S8, Supporting Information).

Table 1: Light scattering parameters of: HRP loaded polymersomes (NR-), HRP loaded polymersomes with inserted OmpF-C (NRC), and HRP loaded polymersomes with inserted OmpF-M (NR+).

	pH 7.4			**pH 6.0**		
	NR-	**NRC**	**NR+**	**NR-**	**NRC**	**NR+**
R_g [nm]	61±8	58±4	61±3	61±1	62±2	63±2
R_h [nm]	64±8	61±4	64±3	66±2	65±2	67±2
ρ []	0.96	0.94	0.95	0.93	0.95	0.93

The ratio (ρ) between the hydrodynamic radius (R_h) and radius of gyration (R_g) was close to 1 indicating that the polymer assemblies have hollow sphere architecture.[57]

TEM micrographs indicate that there were no significant differences in size and architecture between polymersomes loaded with HRP without OmpF (NR-) and those containing HRP with different OmpF mutants inserted (NR+ and NRC) (Figure S10-S12, Supporting Information). The diameter of the polymersomes obtained by TEM is between 50-120 nm, in agreement with the light scattering results (Table 2). In addition, polymersome NRs (without and with inserted OmpF-M/C) were stable at room temperature at both pH 7.4 and 6.0 for several days. Cryo-TEM micrographs clearly indicate that the membrane integrity is preserved upon insertion of OmpF-C, and confirm the size obtained by TEM analysis (Figure 3). Unlike the other methods, cryo-TEM revealed a minor population of worms, but which is not interfering with the bio-valve insertion and functionality.

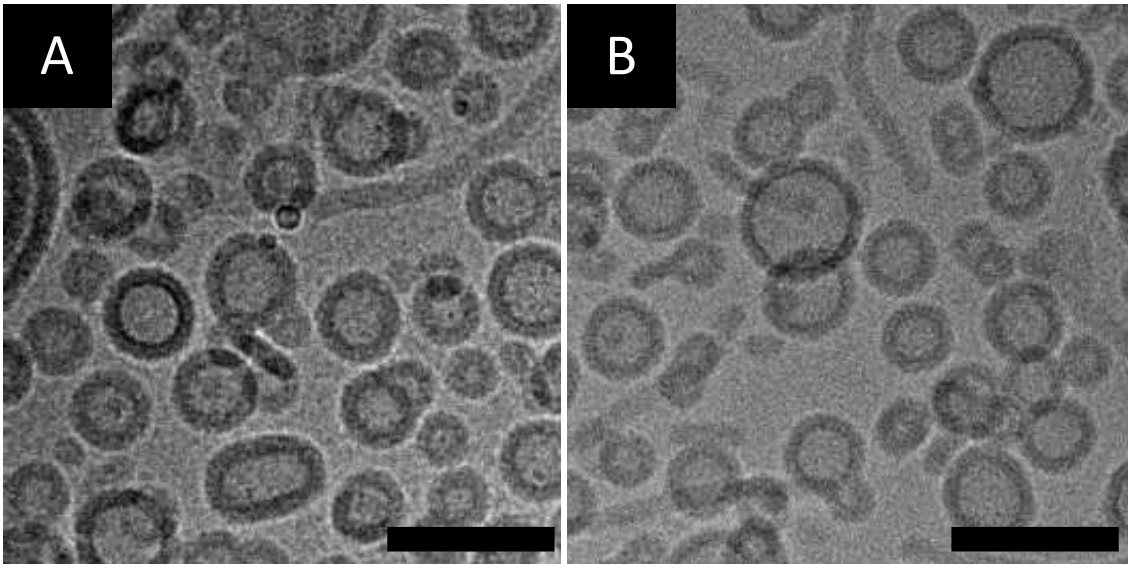

Figure 3: Cryo-TEM micrograph of A) HRP loaded $PMOXA_6$- *b*-$PDMS_{44}$- *b*-$PMOXA_6$ polymersomes equipped with OmpF-C, NRC, and B) HRP loaded $PMOXA_6$- *b*-$PDMS_{44}$- *b*-$PMOXA_6$ polymersomes without OmpF, NR-. Scale bar 100nm.

Before analysing the influence of the pH change on the activity of the catalytic compartments, the behaviour of free HRP was investigated, since enzymes have an optimal pH and a window of operation and stability. HRP presented a pH dependent activity, with an activity significantly higher at pH 6.0 than at pH 7.4 (Figure 4A), but becoming irreversibly deactivated below pH 5.0.[58, 59] Cycling pH changes between 7.4 and 6.0 revealed that the free enzyme lost its activity very fast. Already after the first full cycle of pH change, a drop in activity of the free HRP up to 12.5% of its initial value was observed, and it further decreased after the second complete pH change cycle. The decrease in enzymatic activity of the free HRP was mainly due to the adjustment of pH with small amount of concentrated HCl in order to avoid dilution. A temporary, local pH decrease below the final pH probably deactivated the enzyme[58, 59] (Figure 4C and S13 Supporting Information). There are other factors resulting in a drop of the perceived activity as well, as for example the accumulation of salt and fluorophores after each cycle that contributed to the reduction of the detected fluorescence intensity.

The low activity of the free HRP after the second pH change cycle remained higher at pH 6.0 than at pH 7.4, but the enzyme did not recover (Figure 4B). This significant decrease in free HRP activity indicates the possible effect of harmful conditions in biosystems in the case of the free enzyme, as for example local changes in pH or a proteolytic attack. Therefore it induces the necessity to protect the enzyme when desired applications are planned, and supports our approach of development of catalytic nanocompartments. Catalytic nanocompartments play in biologic conditions a dual role: they shield the enzymes from local harmful conditions and proteolytic attack, whilst allowing them to perform their activity *in situ*.

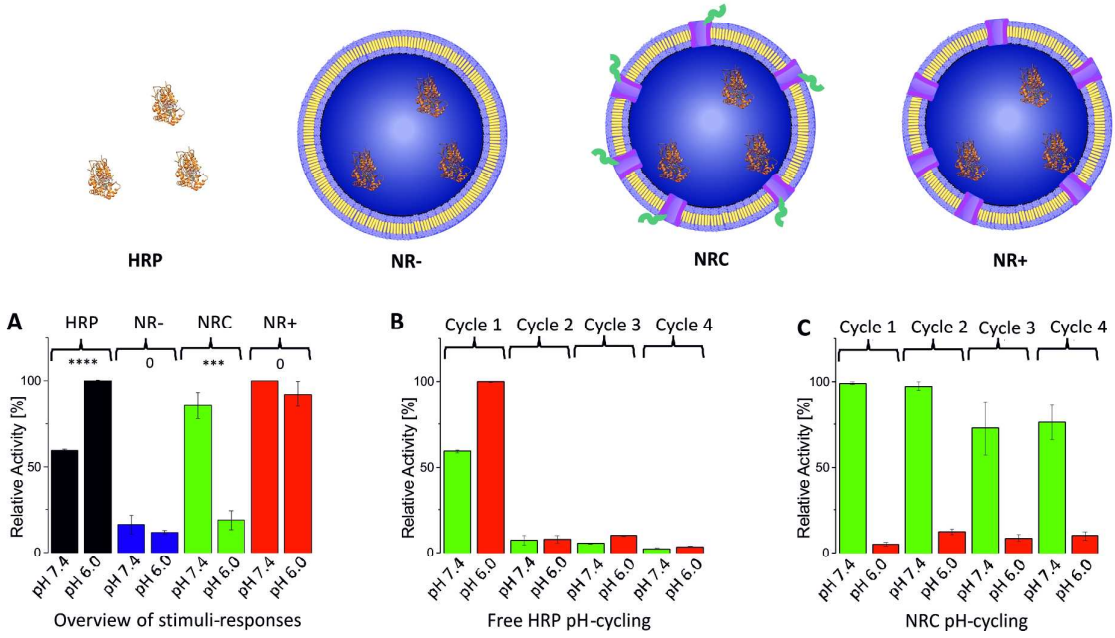

Figure 4. A) Activity of HRP based on the increase in fluorescence intensity of HRP product, measured at pH 7.4 and pH 6: free HRP (black), NR- (blue), NRC (green), and NR+ (red). The stars indicate the statistical significance (P value; Table S6 Supporting Information). B) Free HRP activity after changing the pH from 7.4 to 6.0, and adding Amplex UltraRed® and H_2O_2 in each cycle. Green: pH 7.4 and red: pH 6.0. C) Bio-valve functionality of OmpF-C when inserted into the membrane of HRP loaded polymersomes (NRC) after changing the pH from 7.4 to 6.0, and adding Amplex UltraRed® and H_2O_2 in each cycle. Green: pH 7.4 and red: pH 6.0. The activities were corrected by taking the volume increase into account.

Stimuli responsiveness of the OmpF-C equipped membranes was evaluated by the *in situ* activity of encapsulated HRP at pH 6.0 and 7.4 both after the first pH cycle (Figure 4A), and after several cycles (Figure 4C). The increase of fluorescence intensity associated with the formation of resorufin-derivative inside the cavity of polymersome NRs represents a direct measure for the transmembrane diffusion of the HRP substrate. Polymersomes loaded with

HRP, but without inserted OmpF, (NR-) had a very low residual activity after dialysis, size exclusion chromatography and treatment with proteinase K (Supporting Information polymersome preparation). In order to understand the cause of this residual HRP activity in NR-, interactions of residual HRP traces with the membrane during the polymersomes formation have been evaluated by addition of HRP in the environment of the polymersomes, and subsequent dialysis. Only HRP activity at the detection limit has been observed, which indicates no HRP bound on the external side of the membrane (Figure S14). Therefore, the residual activity of NR- is probably due to the partition of Amplex UltraRed between the aqueous phase and the hydrophobic membrane, resulting in a very small fraction of auto-oxidised Amplex UltraRed in the presence of H_2O_2.

The initial HRP activities of the NRs (NRC, NR-, NR+) were normalised for a simpler comparison, such that the highest activity of NR+ was set to 100%. (Figure 4, Figure S175-18, Table S5, Supporting Information). HRP activity values represent the mean value of three independent measurements. A remarkable stimuli-response of the catalytic compartment containing HRP was observed for a pH change of only 1.4 units: *in situ* HRP activity inside NRC decreased up to 20% of the activity at pH 7.4 upon the decrease of pH at 6.0, thereby changing from an activity close to NR+ to an activity close to the low residual activity of NR- (Figure 4A), completely overriding the pH-dependency of free HRP. This indicates, within the error limits, a change of the OmpF-C pore from an “open state” (pH 7.4) to a “closed state” (pH 6.0) due to a conformational change of Gala3 inside OmpF-C. The pH-responsive change in the accessibility of OmpF-C for molecular diffusion triggered *in situ* HRP activity, and induced a functionality change from an “active” catalytic compartment to a “non-active” one. This pH-dependent behaviour allows the catalytic nanocompartments to start their activity “on demand” by a simple pH change. At pH 6.0, where OmpF-C is in “closed” state, the catalytic compartment has low functionality, even if inside the cavity HRP is active, and expected to have a higher activity compared to that at pH 7.4 (Figure 4A, free HRP and

NRC). On the contrary, when OmpF-C is in an "open" state, substrates pass through the membrane and the functionality of the catalytic compartment is fully restored due to the intrinsic activity of HRP. Interestingly, both the enzyme activity of NRC and that of the catalytic nanocompartment with OmpF-M, NR+, is significantly higher at pH 7.4 than that of the free HRP at this pH, matching the activity value of the free HRP at pH 6.0 (Figure 4A). Note that the increase of the enzyme activity inside the confined space of the polymersome cavity compared with bulk assays was observed in similar conditions (amount of enzyme, ratio of substrates). The increase in activity upon encapsulation of enzymes inside nano-compartments is due to the effect of the confined nano-space, which enhances the interaction of the enzymes with the substrates.[60] Inside the cavity of polymersomes there is an increase in the probability of interaction between the enzyme molecules and their substrates due to an increase of the duration the substrates are remaining in proximity of the enzymes. In addition, the impermeable synthetic membrane allows molecular transport through and thus *in situ* enzymatic reaction when the pores of OmpF-C are open, and serve for a rapid diffusion of substrates/products. We estimated that for a 125nm diameter polymersome the mean number of porin molecules per vesicle is around 11 OmpF molecules/vesicle have been inserted in the conditions we used for OmpF insertion (Supporting Information).

The stimuli response behaviour of OmpF-C inserted in polymersome membranes was reproducible (raw data: Figure S15-S19, Table S5 Supporting Information). The OmpF pore with a 600 Da molecular weight cut-off allowed Amplex (300 Da) to pass through in its "open state" despite being modified with a 1322.4 Da Gala3 peptide, which indicates that Gala3 is extended outside of the pore at pH 7.4. Various molecular factors might be responsible for the bio-valve functionality of Gala3 inside the OmpF pore: change in the peptide protonation state, change in the peptide conformation, and different electrostatic interactions within the pore. Based on average pKa-values, it can be estimated that at pH 6.0 only around 2% of the glutamic acid groups would become protonated. Therefore, this change in the protonation

state of the Gala3-peptide is not the key parameter affecting the transport through the OmpF pore, being insufficient to explain the significant change in the *in situ* HRP activity (Figure S22, Table S8 Supporting Information). However, significant structural changes have been reported for the GALA-peptide: GALA is in a random coil at pH 7.4 and forms anα-helix at pH 5.5.[48] We believe that even the short Gala3-peptide undergoes similar conformational changes in combination with interactions between GALA3 in the double mutant.

Catalytic compartments containing HRP and equipped with OmpF-M were still active after two weeks, which is a remarkable improvement in the stability of encapsulated HRP compared with the free enzyme (Figure S20, Supporting Information) The reversibility of the stimuli response of NRC was evaluated by cycling the pH change, and measuring the HRP activity triggered by these cycles. (Figure 4C). With each pH cycle, new Amplex UltraRed® and H_2O_2 were added. Each time, upon a pH increase to 7.4, the NRC activity increased due to the opening of the OmpF-C pore, and inversely the activity decreased when the pH was decreased to 6.0, because the OmpF pore was closed. The activity of NRC at pH 7.4 on the fourth cycle slightly decreased to 75%, which can be explained by saturation effects resulting from successive additions of the substrate and salts[61, 62]. In comparison free HRP significantly decreased its activity in bulk after the first cycle (Fig S13). Therefore, our NRC is not only a reversible pH catalytic compartment, but also an ideal candidate to protect the enzymes and preserve their activity. Moreover, when compared to the time resolution of the enzyme kinetic, the change between open/closed states can be considered instantaneous.

We successfully developed catalytic compartments with reversible triggered activity by inserting bio-valves in the membrane of synthetic compartments loaded with enzymes. The role of the bio-valves is to control the *in situ* activity inside catalytic nanocompartments by changing in a reversible manner from an “open” to a “close” state that controls the molecular flow through the compartment membrane. The bio-valve resulted from attachment of stimuli-

responsive peptides to a genetically modified channel porin, OmpF. Changes in the conformation inside the pores, upon a pH change of 1.4 units in the environment of the nanocompartments block/unblock the pores of OmpF in a reversible manner. The pH-reversible bio-valve functionality induced an *in situ* activity switch on/off by the molecular flow of substrates/products through the polymersome membrane. Compared to all stimuli-responsive compartments reported, which either change their integrity or do not allow a controlled permeability, our synthetic compartments equipped with a genetically engineered bio-valve represent a step beyond what has been achieved to date in complex functionality. In addition, the encapsulation of the enzyme served both to increase the activity due to the confined reaction space inside the polymersomes, and to increase its stability compared to the free enzyme. We anticipate that further improvements to the system can be made by: i) expanding it for other types of stimuli associated with attachment of corresponding molecular groups, and ii) adjustment of the number and length of the stimuli responsive molecules to modulate the molecular flow through the pores.

Our strategy to build catalytic compartments with reversible triggered functionality has the potential to completely change the manner in which stimuli-responsive compartments are developed in the future, especially but not limited to medical or catalysis applications. In addition, the insertion of reversible bio-valves in synthetic membranes is not limited to nanocompartments and can be easily expanded to planar membranes, resulting in a wide range of applications ranging from analytical chemistry, nanofiltration, and up to medicine.

Methods. A detailed description of the reagents is found before each experimental section in the Supporting Information. The double cysteine mutant K89C R270C of OmpF-WT (OmpF-M) was created to introduce thiol groups as anchor points for the attachment of stimuli responsive peptides. K89 C represents one lysine in 89th position, which is replaced by a

cysteine, whilst R270C represents one ariginine replaced by a cysteine. The plasmid bearing the OmpF-gene used in this work has been previously described.[63] Mutations were introduced via site-directed mutation directly on the plasmid, by using a two-step PCR protocol[64] adapted for the PfuTurbo DNA Polymerase (Agilent) and the corresponding primers (Table S1, Supporting Information). The amplicon was then purified on a 1% agarose gel using a gel-extraction kit from QIAGEN. The amplicon was first transfected to XL1-Blue ultra-competent cells, then extracted and sequenced prior to transfection into BL21 (DE3)Omp8.[63] This intermediate step over the ultracompetent cells was necessary to improve uptake because the amplicon was significantly larger than the supercoiled plasmid.

Both OmpF-WT and the OmpF mutants (single mutants K89C-OmpF, R270C-OmpF, and the double mutant K89C-R270C-OmpF) were expressed following a published procedure[55], with minor changes (see Supporting Information). The extraction of OmpF was made in PBS buffer containing octylglucopyranoside (3 w/w % OG; Affymetrix). The purity of OmpF was evaluated on a 12% SDS-PAGE gel, and the concentration of OmpF was measured spectrometrically at λ = 280 nm with Nanodrop (Witec Ag), and with a BCA-protein assay (Thermo Fischer Scientific)

A DMSO solution of 20eq. Gala3 peptide-maleic imide per cysteine-group was slowly added to 1mL OmpF-M (1g/L) in PBS with 3 w/w % OG at pH=7.4, and stirred overnight at room temperature. OmpF-C was dialysed twice against 1L PBS containing 0.5 w/w % OG using Midi GeBAflex-tube (50-800µL; 6-8kDa MWCO). The solution was concentrated 2x using 10kDa Amicon Centrifugal Filters (Milipore).

The protein concentration was measured spectrometrically at λ = 280 nm with Nanodrop (Witec Ag), and the labelling efficiency was evaluated by using the acrylodane assay (details in Supporting Information), and mass spectrometry (applying SDS-gel for purification; in-gel digestion and HPLC-ESI MS on the extract).[65]

Polymersomes either without and in the presence of biomolecules (OmpF and HRP) were prepared by the film rehydration method of $PMOXA_6$-*b*-$PDMS_{44}$-*b*-$PMOXA_6$ triblock copolymer (details in Supporting Information).[66] After confirming the purity and homogeneity of the polymersomes using a Malvern Zetasizer (PDI < 0.1), the polymersome concentration of different samples has been adjusted to avoid differences by comparing their ability to scatter light with a Spectramax M5 spectrophotometer in semi-micro PS cuvettes (VWR).

Light scattering experiments were performed using an ALV goniometer (ALV GmbH, Germany) equipped with an ALV He –Ne laser (JDS Uniphase, wavelength λ = 632.8 nm). The solutions after film rehydration method (polymer concentration diluted to 1.25, 0.625, 0.313 and 0.156 g/L) were measured in a 10mm cylindrical quartz cell at angles ranging from 30° to 150° at 293 K with angular steps of 10°. ALV/Static & Dynamic FIT and PLOT program version 4.31 10/10 were used for data analysis. Static light scattering data were processed according to the Guinier-model.

Polymersome solutions were diluted to a polymer concentration of 0.05 g/L and 5 µL were negatively stained with 2% uranyl acetate solution and deposited on a carbon-coated copper grid. The samples were examined with a transmission electron microscope (Philips CM-100) operated at 80 kV.

The activity of HRP (free and encapsulated into polymersomes equipped with or without OmpF-C or OmpF-M,) was measured using Amplex UltraRed® (Invitrogen) as substrate (500uM final concentration) and hydrogen peroxide as co-substrate (13.3uM final concentration). The HRP reaction was evaluated at pH 7.4 and 6.0. HRP activity was measured in: i) free conditions, ii) polymersomes equipped with peptide bearing OmpF-M, (NRC), iii) polymersome containing HRP without inserted OmpF, (NR-), and iv) polymersomes containing HRP and with OmpF-C inserted in the membrane, (NR+).

For each resulting kinetic curve based on the increase of the fluorescence intensity of the resorufin-derivative over time, the initial slope of the graph (0 to 200s) was taken as the initial activity and all values were normalised, such that the value corresponding to NR+ was set to 100%. For the reversibility experiments, pH was adjusted with minimal amounts of concentrated hydrochloric acid or sodium hydroxide. HRP reaction was detected at pH 7.4, then the pH was decreased to 6.0 and another equivalent of Amplex UltraRed® and hydrogen peroxide were added and the fluorescence intensity of the resorufin-derivative was measured again. Then the pH was increased back to 7.4 to continue with the next cycle.

Acknowledgements

The Swiss National Science Foundation, NCCR Molecular Systems Engineering, The Swiss Nanoscience Institute, and the University of Basel are acknowledged for financial support. C. Edlinger thanks Dr. Stefan Nicolet and Dr. Marc Creus (University of Basel) for support in the genetic engineering, Dr. Alexander Schmidt (University of Basel) for mass spectroscopy experiment, Dr. Adrian Dinu (University of Basel) for supplying the PMOXA-*b*-PDMS-*b*-PMOXA, and Gabriele Persey (University of Basel) for TEM. Dr. Ozana Fischer (University of Basel) is acknowledged for initiating this project and supplying Omp8, and Dr. M. Chami (University of Basel, C-CINA) for the cryo-TEM experiments. The authors thank Mr. David Hughes for editing the manuscript.

ASSOCIATED CONTENT

The Supporting Information is available free of charge on the ACS Publications website at DOI:

Supporting information: detailed description of the experimental methods; additional data including DNA-sequencing; SDS-gels; DOL-measurements of the OmpF-conjugate; TEM-

and LS-data; enzyme and catalytic nanocompartments kinetics; ANOVA and calculations of number of OmpF/polymersome.

References

1. Watson, H. *Essays Biochem.* **2015,** 59, 43-69.
2. Ranade, S. S.; Syeda, R.; Patapoutian, A. *Neuron* **2015,** 87, 1162-1179.
3. Gautier, A.; Gauron, C.; Volovitch, M.; Bensimon, D.; Jullien, L.; Vriz, S. *Nat Chem Biol* **2014,** 10, 533-541.
4. Zhang, C.; McAdams, D. A.; Grunlan, J. C. *Adv Mater* **2016,** 28, 6292-6321.
5. Palivan, C. G.; Goers, R.; Najer, A.; Zhang, X.; Car, A.; Meier, W. *Chem Soc Rev* **2016,** 45, 377-411.
6. Garni, M.; Thamboo, S.; Schoenenberger, C.-A.; Palivan, C. G. *Biochim. Biophys. Acta, Biomembr.*
7. Presley, A. D.; Chang, J. J.; Xu, T. *Soft Matter* **2011,** 7, 172-179.
8. Tanner, P.; Egli, S.; Balasubramanian, V.; Onaca, O.; Palivan, C. G.; Meier, W. *FEBS Letters* **2011,** 585, 1699-1706.
9. Thingholm, B.; Schattling, P.; Zhang, Y.; Städler, B. *Small* **2016,** 12, 1806-1814.
10. Tu, Y.; Peng, F.; Sui, X.; Men, Y.; White, P. B.; van Hest, J. C. M.; Wilson, D. A. *Nat Chem* **2016,** advance online publication.
11. LeDuc, P. R.; Wong, M. S.; Ferreira, P. M.; Groff, R. E.; Haslinger, K.; Koonce, M. P.; Lee, W. Y.; Love, J. C.; McCammon, J. A.; Monteiro-Riviere, N. A.; Rotello, V. M.; Rubloff, G. W.; Westervelt, R.; Yoda, M. *Nat Nano* **2007,** 2, 3-7.
12. Dinu, M. V.; Spulber, M.; Renggli, K.; Wu, D.; Monnier, C. A.; Petri-Fink, A.; Bruns, N. *Macromol Rapid Comm* **2015,** 36, 507-514.
13. Langowska, K.; Kowal, J.; Palivan, C. G.; Meier, W. *J. Mater. Chem. B* **2014,** 2, 4684-4693.
14. Zhang, X.; Lomora, M.; Einfalt, T.; Meier, W.; Klein, N.; Schneider, D.; Palivan, C. G. *Biomaterials* **2016,** 89, 79-88.
15. Xie, W.; He, F.; Wang, B.; Chung, T.-S.; Jeyaseelan, K.; Armugam, A.; Tong, Y. W. *J. Mater. Chem. A* **2013,** 1, 7592-7600.
16. Che, H.; van Hest, J. C. M. *J. Mater. Chem. B* **2016,** 4, 4632-4647.
17. Dobrunz, D.; Toma, A. C.; Tanner, P.; Pfohl, T.; Palivan, C. G. *Langmuir* **2012,** 28, 15889-99.
18. Spulber, M.; Baumann, P.; Saxer, S. S.; Pieles, U.; Meier, W.; Bruns, N. *Biomacromolecules* **2014,** 15, 1469-1475.
19. Tanner, P.; Balasubramanian, V.; Palivan, C. G. *Nano Lett* **2013,** 13, 2875-2883.
20. Godoy-Gallardo, M.; Labay, C.; Jansman, M. M. T.; Ek, P. K.; Hosta-Rigau, L. *Adv. Healthcare Mater.* **2016**, 1601190-n/a.
21. Balasubramanian, V.; Correia, A.; Zhang, H.; Fontana, F.; Mäkilä, E.; Salonen, J.; Hirvonen, J.; Santos, H. A. *Adv Mater* **2017**, 1605375-n/a.
22. Bermudez, H.; Brannan, A. K.; Hammer, D. A.; Bates, F. S.; Discher, D. E. *Macromolecules* **2002,** 35, 8203-8208.
23. Wu, D.; Spulber, M.; Itel, F.; Chami, M.; Pfohl, T.; Palivan, C. G.; Meier, W. *Macromolecules* **2014,** 47, 5060-5069.
24. Le Meins, J. F.; Sandre, O.; Lecommandoux, S. *Eur. Phys. J. E* **2011,** 34, 1-17.
25. Brinkhuis, R. P.; Rutjes, F. P. J. T.; van Hest, J. C. M. *Polym. Chem.* **2011,** 2, 1449-1462.
26. Liu, F.; Eisenberg, A. *J Am Chem Soc* **2003,** 125, 15059-15064.
27. Anajafi, T.; Mallik, S. *Ther. Delivery* **2015,** 6, 521-534.

28. Kuiper, S. M.; Nallani, M.; Vriezema, D. M.; Cornelissen, J. J. L. M.; van Hest, J. C. M.; Nolte, R. J. M.; Rowan, A. E. *Org Biomol Chem* **2008,** 6, 4315-4318.
29. Vriezema, D. M.; Hoogboom, J.; Velonia, K.; Takazawa, K.; Christianen, P. C. M.; Maan, J. C.; Rowan, A. E.; Nolte, R. J. M. *Angew. Chem. Int. Ed.* **2003,** 42, 772-776.
30. Gaitzsch, J.; Appelhans, D.; Wang, L.; Battaglia, G.; Voit, B. *Angew. Chem. Int. Ed.* **2012,** 51, 4448-4451.
31. Spulber, M.; Najer, A.; Winkelbach, K.; Glaied, O.; Waser, M.; Pieles, U.; Meier, W.; Bruns, N. *J Am Chem Soc* **2013,** 135, 9204-9212.
32. Edlinger, C.; Zhang, X.; Fischer-Onaca, O.; Palivan, C. G., Polymer Nanoreactors. In *Encycl. Polym. Sci. Eng.*, John Wiley & Sons, Inc.: 2013.
33. Meier, W.; Nardin, C.; Winterhalter, M. *Angew.e Chem.-Int. Ed.* **2000,** 39, 4599-+.
34. Lomora, M.; Garni, M.; Itel, F.; Tanner, P.; Spulber, M.; Palivan, C. G. *Biomaterials* **2015,** 53, 406-414.
35. Lomora, M.; Dinu, I. A.; Itel, F.; Rigo, S.; Spulber, M.; Palivan, C. G. *Macromol Rapid Comm* **2015,** 36, 1929-1934.
36. Einfalt, T.; Goers, R.; Dinu, I. A.; Najer, A.; Spulber, M.; Onaca-Fischer, O.; Palivan, C. G. *Nano Lett* **2015,** 15, 7596-7603.
37. Muhammad, N.; Dworeck, T.; Fioroni, M.; Schwaneberg, U. *J. Nanobiotechnol* **2011,** 9, 8.
38. Ihle, S.; Onaca, O.; Rigler, P.; Hauer, B.; Rodriguez-Ropero, F.; Fioroni, M.; Schwaneberg, U. *Soft Matter* **2011,** 7, 532-539.
39. Kocer, A.; Walko, M.; Feringa, B. L. *Nat. Protocols* **2007,** 2, 1426-1437.
40. Onaca, O.; Sarkar, P.; Roccatano, D.; Friedrich, T.; Hauer, B.; Grzelakowski, M.; Güven, A.; Fioroni, M.; Schwaneberg, U. *Angew. Chem. Int. Ed.* **2008,** 47, 7029-7031.
41. Guven, A.; Fioroni, M.; Hauer, B.; Schwaneberg, U. *J. Nanobiotechnol* **2010,** 8, 14.
42. Jung, Y.; Bayley, H.; Movileanu, L. *J Am Chem Soc* **2006,** 128, 15332-15340.
43. Loudwig, S.; Bayley, H. *J Am Chem Soc* **2006,** 128, 12404-12405.
44. Banghart, M. R.; Volgraf, M.; Trauner, D. *Biochemistry-Us* **2006,** 45, 15129-15141.
45. Bieligmeyer, M.; Artukovic, F.; Nussberger, S.; Hirth, T.; Schiestel, T.; Müller, M. *Beilstein J. Nanotechnol.* **2016,** 7, 881-892.
46. Koebnik, R.; Locher, K. P.; Van Gelder, P. *Mol Microbiol* **2000,** 37, 239-253.
47. Itel, F.; Najer, A.; Palivan, C. G.; Meier, W. *Nano Lett* **2015,** 15, 3871-8.
48. Lin, B. F.; Missirlis, D.; Krogstad, D. V.; Tirrell, M. *Biochemistry-Us* **2012,** 51, 4658-4668.
49. Jackson, M. E.; Pratt, J. M.; Stoker, N. G.; Holland, I. B. *The EMBO Journal* **1985,** 4, 2377-2383.
50. Yang, Z. H.; Attygalle, A. B. *J Mass Spectrom* **2007,** 42, 233-243.
51. Lang, S.; Spratt, D. E.; Guillemette, J. G.; Palmer, M. *Anal. Biochem.* **2005,** 342, 271-279.
52. Griffin, N. M.; Schnitzer, J. E. *Mol. Cell. Proteomics* **2011,** 10, R110.000935.
53. Chen, H.; Ahsan, S. S.; Santiago-Berrios, M. E. B.; Abruña, H. D.; Webb, W. W. *J Am Chem Soc* **2010,** 132, 7244-7245.
54. Kawski, A.; Bojarski, P.; Kuklinski, B. *Z Naturforsch A* **2002,** 57, 94-97.
55. Grzelakowski, M.; Onaca, O.; Rigler, P.; Kumar, M.; Meier, W. *Small* **2009,** 5, 2545-2548.
56. Seddon, A. M.; Curnow, P.; Booth, P. J. *Biochim. Biophys. Acta, Biomembr.* **2004,** 1666, 105-117.
57. Zhang, Y. J.; Guan, Y.; Yang, S. G.; Xu, J.; Miao, X. P.; Cao, W. X. *Chinese J Polym Sci* **2004,** 22, 111-115.
58. Bamdad, K.; Ranjbar, B.; Naderi-Manesh, H.; Sadeghi, M. *EXCLI Journal* **2014,** 13, 611-622.
59. Chattopadhyay, K.; Mazumdar, S. *Biochemistry-Us* **2000,** 39, 263-270.
60. Baumann, P.; Spulber, M.; Fischer, O.; Car, A.; Meier, W. *Small* **2017**, 1603943-n/a.
61. Esteves, V. I.; Santos, E. B. H.; Duarte, A. C. *J Environ Monitor* **1999,** 1, 251-254.
62. Warren, J. C.; Cheatum, S. G. *Biochemistry-Us* **1966,** 5, 1702-&.
63. Prilipov, A.; Phale, P. S.; Van Gelder, P.; Rosenbusch, J. P.; Koebnik, R. *Fems Microbiol Lett* **1998,** 163, 65-72.
64. Wang, W. Y.; Malcolm, B. A. *Biotechniques* **1999,** 26, 680-682.

65. Glatter, T.; Ludwig, C.; Ahrné, E.; Aebersold, R.; Heck, A. J. R.; Schmidt, A. *J. Proteome Res.* **2012,** 11, 5145-5156.
66. Itel, F.; Chami, M.; Najer, A.; Lörcher, S.; Wu, D.; Dinu, I. A.; Meier, W. *Macromolecules* **2014,** 47, 7588-7596.

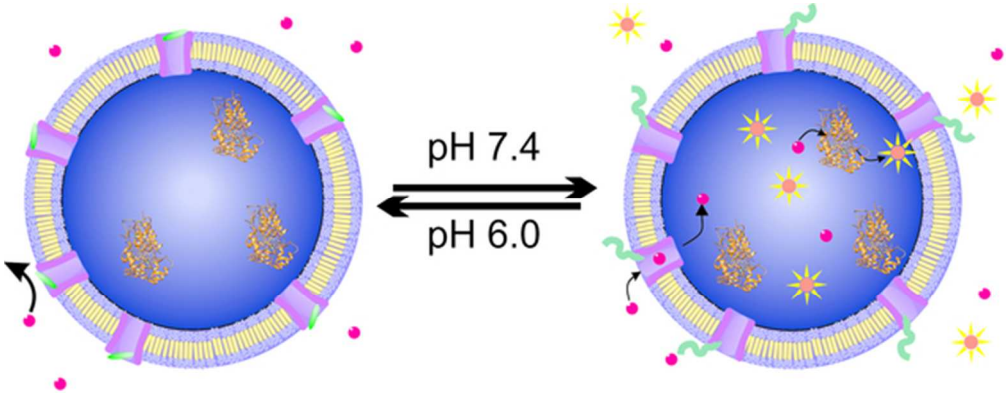

TOC only.

53x20mm (300 x 300 DPI)